Electronic Supplementary Information

Ratiometric Fluorescent and Colorimetric Dual-Modal Sensing Strategy for Discrimination and Detection of D_2O from H_2O

Jingda Liu, [a] Xinyu Ma, [b] Qi Song, [a] Junying Zang, [a] Jingcheng Hao, [a] Weisheng Liu, [b] and Jie Jiang [a, c]*

[a] Key Laboratory of the Colloid and Interface Chemistry of the Ministry of Education, School of Chemistry and Chemical Engineering, Shandong University, Jinan, 250100, China.

[b] State Key Laboratory of Applied Organic Chemistry, Key Laboratory of Nonferrous Metal Chemistry and Resources Utilization of Gansu Province, and College of Chemistry and Chemical Engineering, Lanzhou University, Lanzhou, 730099, China.

[c] Shenzhen Research Institute of Shandong University, Shenzhen 518057, P. R. China.

Corresponding author. *Email: jiejiang@sdu.edu.cn

Table of Contents

Experimental Procedures

1. General Information

All reagents and solvents were obtained commercially and used without further purification unless otherwise noted. Analytical thin-layer chromatography (TLC) was performed on a silica gel plate and analyzed by UV light or by potassium permanganate stains followed by heating. Flash chromatography was carried out utilizing silica gel (200-300 mesh). ^{1}H NMR and ^{13}C NMR spectra were recorded in DMSO-d_6 at room temperature on a Bruker AM-400 spectrometer (400 MHz ^{1}H, 100 MHz ^{13}C) unless other noted. Data for ^{1}H NMR are reported as follows: chemical shift (δ ppm), multiplicity (s = singlet, d = doublet, t = triplet, m = multiplet, dd = doublet doublet), coupling constants (Hz), integration. Data for ^{13}C NMR are reported as chemical shifts. HRMS were performed on a Bruker Apex II mass instrument (ESI).

All UV-visible spectra and fluorescence spectra were recorded using a Hitachi UV-2910 spectrophotometer and Hitachi F-7100 luminescence spectrometer, respectively. All fluorescence lifetime measurements were recorded by using the FLIM equipment consisting of the confocal optical microscope (Nanofinder FLEX2, Tokyo Instruments, Inc.) and a time-correlated single-photon counting (TCSPC) module (Becker & Hickl, SPC-150). Fluorescent quantum yields were determined to be 0.04% for **HTI** in H_2O, and 1.56% in D_2O, respectively by an absolute method using an integrating sphere on FLS920 of Edinburgh Instrument.

2. General Procedure for Preparation of Compound HTI and MTI

Scheme S1. Synthesis of **HTI**.

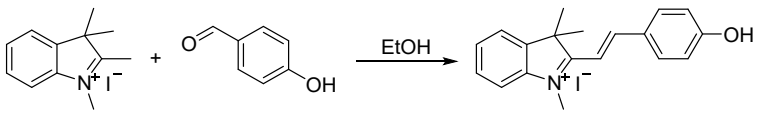

HTI

2-[(*E*)-2-(4-hydroxyphenyl)ethenyl]-1,3,3-trimethyl-3*H*-indol-1-ium iodide (HTI)

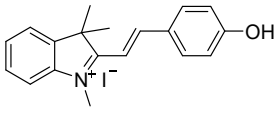

1,2,3,3-tetramethyl-3H-indoleiodide (903.5 mg, 3.0 mmol) and *p*-hydroxybenz-aldehyde (439.6 mg, 3.6 mmol) were added into 40 mL ethanol in a 100 mL Schlenk flask. The mixture was stirred and refluxed for 12h under an argon atmosphere. The process of the reaction was monitored by thin-layer chromatography (TLC). After cooling to room temperature, the reaction mixture was filtered, washed

with petroleum ether, and dried to afford an orange-red solid, no further purification was needed (968.8 mg, 79.7%). The NMR data is agreed with that in the previously reported literature.[1]

Scheme S2. Synthesis of **MTI**.

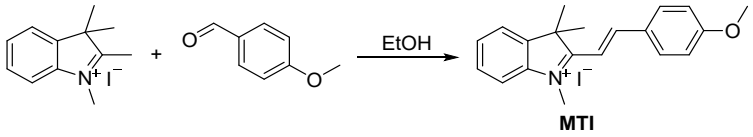

(E)-2-(4-methoxystyryl)-1,3,3-trimethyl-3H-indol-1-ium (MTI)

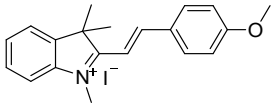

The synthesis of **MTI** was performed according to the reported literature by using 1,2,3,3-tetramethyl-3H-indoleiodide (903.5 mg, 3.0 mmol) and 4-methoxybenzaldehyde (489.6 mg, 3.6 mmol) with a yield of 72.6%.[2]

3. Experimental Section

3.1 General Procedure for Sensing Studies

Stock solutions of **HTI** and **MTI** (10 mM) were prepared in DMSO. Freshly prepared **HTI** or **MTI** (4 μL) was diluted to 20 μM to collect the spectrum at room temperature. Solutions of NaCl, KCl, $CaCl_2$, $Mg(ClO_4)_2$, $Zn(ClO_4)_2$, $Cu(ClO_4)_2$, and Na_2SO_4 were prepared by dissolving their salts into distilled water.

D_2O and distilled H_2O samples were commercially available and stored in either glass or plastic bottles. Before the discrimination experiment and quantitative analysis measurement, freshly opened D_2O and H_2O were distilled and subsequently treated with degas and protection with N_2 atmosphere and stored in glass vessels.

3.2 Detailed Protocols for pH Effects

Different pH values of Britton–Robinson (B–R) buffer (pH 3.00 – 11.00) were prepared. The solution for spectroscopic determination was obtained by diluting 4 μL of the stock solution to get a 20 μM solution in different pH of B–R buffer.

3.3 ^{1}H NMR Titration

^{1}H NMR spectrum was sequentially recorded for **HTI** (15 mg, 0.037 mmol) dissolved in DMSO-d_6 (0.6 mL), followed by the addition of 10 eq Et_3N (0.37 mmol, 51.3 μL) to adjust the pH value of the above solution, and further treated with 20 eq HCl (0.74 mmol, 64.5 μL) to reinstall the pH value.

3.4 ^{1}H NMR of HTI in D_2O and H_2O

^{1}H NMR of **HTI** (0.2 mM) was conducted in degassed pure H_2O and D_2O (0.5 mL, containing 1% DMSO as cosolvent) with D_2O as an external standard.

3.5 NaOH, DCl, and HCl Titration Experiment

Freshly prepared NaOH (0.1 M in H_2O, 0 – 6 μL) was added to a solution of **HTI** in H_2O (20 μM). Both absorption and fluorescence spectra were collected after each addition. Similar experiments were conducted by titrating freshly prepared DCl (0.1 M, 0 – 5 μL) or HCl (0.1 M, 0 – 5 μL) into the D_2O solution of **HTI** (20 μM), respectively.

4. Determination of the pK_a of Sensor HTI

The pKa value of **HTI** was determined by the Henderson-Hasselbalch equation:[2]

$$\log[(R_{max} - R)/(R - R_{min})] = pK_a - pH$$

Where R is the fluorescence intensity ratio between 558 and 540 nm, R_{max} (or R_{min}) is the corresponding maximum (or minimum) limiting values of R. R represents the observed value. The pK_a value was then calculated based on the plots of $\log[(R_{max} - R)/(R - R_{min})]$ vs. pH as shown in Fig. 2e.

Based on the experiment on the pH effect on emission, the pK_a value of **HTI** was calculated to be 7.11 in the B–R buffer (containing 0.2 % DMSO) system.

5. Determination of the Detection Limit

The detection limit was calculated based on the fluorescence and absorption titration, respectively. Fluorescence emission spectrum or absorption of sensor **HTI** in D_2O solution was measured by thirty times and the standard deviation (σ) of this blank measurement was achieved. The slope (k) was derived from the calibration curve for quantitative analysis of H_2O. The detection limit was determined with the following equation:[3]

$$\text{Detection limit} = 3\sigma/k.$$

Based on the absorption titration experiment shown in Fig. 4a and 4b, the detection limit value of H_2O was calculated to be 0.196% in D_2O (containing 0.2% DMSO).

$$\text{Detection limit of } H_2O = 3^* \, 0.000778/1.19258 = 0.001958 = 0.196\% \text{ (v/v)}$$

Based on the fluorescence titration experiment shown in Fig. 4c and 4d, the detection limit value of H_2O was calculated to be 0.738% in D_2O (containing 0.2% DMSO).

$$\text{Detection limit of } H_2O = 3^* \, 0.002373/0.97188 = 0.00732 = 0.732\% \text{ (v/v)}$$

A similar method was performed to determine the detection limit of D_2O in H_2O according to the data in Fig. 5 of the main article.

Based on the absorption titration experiment shown in Fig. 4a and 4b, the detection limit value of D_2O

was calculated to be 0.597% in H_2O (containing 0.2% DMSO).

Detection limit of D_2O = 3*0.002373/1.19258 = 0.005969 = 0.597% (v/v)

Based on the fluorescence titration experiment shown in Fig. 4c and 4d, the detection limit value of D_2O was calculated to be 1.604% in H_2O (containing 0.2% DMSO).

Detection limit of D_2O = 3*0.00516/0.97188 = 0.01593 = 1.593% (v/v)

6. Spiked Recovery Experiments

Spiked recovery experiments were carried out based on the absorption method. Firstly, freshly prepared D_2O and H_2O were degassed and protected with N_2, which were mixed to obtain different fractions of H_2O in 2 mL of D_2O-H_2O solution in total, labeled as samples 1 – 8, and the content was labeled as "spiked%", as shown in Table S1.

HTI (4 μL) was added to 2 mL of the above samples (1-8) to collect the absorption spectrum at room temperature. The absorption ratio ($A_{520\ nm}/A_{452\ nm}$) was determined to be the value y for each sample, which could be used to calculate the value x based on the linear relationship from Fig. 4b:

$$y = 1.19258\ x + 1.05082$$

The data list in Table 1 in the main manuscript was calculated using the following equation:

For samples 1-4,

Measured% = x × 100;

For samples 5-8,

Measured% = (1 – x) × 100.

Recovery% = (Measured%/Spiked%) × 100

7. Additional Discussion

Our mechanism for distinguishing D_2O from H_2O was based on their alkaline difference, and therefore the pH/pD values should be consistent for the used samples. As known, CO_2 can be easily adsorbed in either H_2O or D_2O, which is assumed as the major interference to the pH/pD values of pure H_2O or D_2O. In our sensing strategy, each H_2O and/or D_2O sample was degassed and measured under an N_2 atmosphere, which fully eliminated the artifacts induced by H_2CO_3. We would like to make some additional discussion as follows:

7.1 Evaluating the pH/pD Control of Used Samples

Firstly, we compared the **HTI** spectroscopy in a freshly opened D_2O solution with that in a pretreated sample. Two parallel experiments were studied by using different branding D_2O samples. For freshly opened D_2O samples, different spectroscopies of **HTI** were noticed between different brands (Fig. S10a and S10c), while the spectra became consistent after these samples were treated with the degas technique (Fig. S10b and S10d). These results suggested

that the pH(pD) values of D_2O were almost consistent in the samples used in our measurements.

Furthermore, we carried out three sets of parallel experiments: Measuring the spectra of **HTI** in three different batches of H_2O and D_2O samples which were stored in vessels of different brands. The very consistent absorption and emission spectra of **HTI** in either H_2O or D_2O were noticed in all three parallel experiments (Fig. S11), further confirming the consistent pH(pD) values of H_2O or D_2O samples could be obtained.

Even though all the above D_2O and H_2O samples were stored in different bottles, pretreated in different vessels, and measured separately, consistent results were obtained for either H_2O or D_2O. The results further demonstrated the reliability of our strategy.

7.2 D_2O and H_2O Samples at Different pH

Since the mechanism for distinguishing D_2O from H_2O is based on the alkaline difference between these two pure samples, these probes including our probe **HTI** and other previously reported probes [3-5] might not be suitable for the discrimination of D_2O from H_2O at different pH/pD values.

7.3 Buffered H_2O and D_2O Samples

HTI was studied in buffered H_2O and D_2O by using the same portion of buffer components of Na_2HPO_4-KH_2PO_4 (10 mM, 1:1). As shown in Fig. S12, **HTI** displayed almost similar spectral properties in either buffered H_2O or D_2O.[6] This is because, unlike neat H_2O and D_2O that possess different pH/pD values, buffered D_2O and H_2O in Na_2HPO_4-KH_2PO_4 displayed almost the same pH/pD value (ΔpH (D) = 0.05, pH = 7.0) according to previous work from Rubinson's group. In this case, the buffered D_2O and H_2O in Na_2HPO_4-KH_2PO_4 would not be suitable for our study on the discrimination of D_2O from H_2O.

Advantages of this work:

In this work, H_2O and D_2O samples were degassed and protected with an N_2 atmosphere to fully eliminate the pH/pD variation induced by CO_2-adsorption, which has been proven to provide consistent pH/pD values of each used sample. We believe this work could provide a more reliable method for discrimination and detection of D_2O and H_2O compared with previously reported probes (*Angew. Chem. Int., Ed*. 2019, *58*, 6280–6284; *Chem. Commun.*, 2020, *56*, 1191–1194; *Microchem. J.* 2022, *176*, 107244.).

Supplementary Figures and Tables

Table S1. Preparation of samples 1-8 for spiked recovery experiments.

Sample (Total 2 mL)	**1**	**2**	**3**	**4**	**5**	**6**	**7**	**8**
V_{H2O} (mL)	0.06	0.10	0.14	0.20	1.94	1.90	1.86	1.80
V_{D2O} (mL)	1.94	1.90	1.86	1.80	0.06	0.10	0.14	0.20
Spiked%	97.0 [a]	95.0 [a]	93.0 [a]	90.0 [a]	97.0 [b]	95.0 [b]	93.0 [b]	90.0 [b]

[a] $V_{D2O}/V_{D2O+H2O;}$ [b] $V_{H2O}/V_{D2O+H2O.}$

Table S2. Comparison of reported organic optical sensors for D_2O/H_2O discrimination.

Sensor	LR [a] (vol%)	LOD (vol%)[b] Trace H_2O in D_2O	Solvent	Sensing response	Detection interferenced by CO_2-induced pH changes.	Reference
NIM-2F 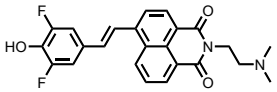	0 – 50.0	0.24	DMSO/D_2O (20:3, v/v)	Single-modal Colorimetric changes	Yes	[3]
AF 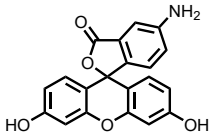	0 – 47.1	0.080	DMSO/D_2O (20:1.8, v/v)	Dual-modal Ratiometric fluorescent/colorimetric changes $I_{412\ nm}/I_{539\ nm}$; $A_{344\ nm}$ /$A_{513\ nm}$	Yes	[3]
CF-D_2O 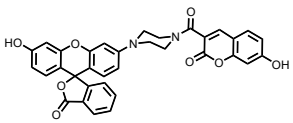	0 – 100	0.165 (I_{450}) 1.05 (I_{550})	0.33% DMSO	Single-modal Turn on response at $I_{450\ nm}$ and $I_{550\ nm}$	Yes	[4]
ES 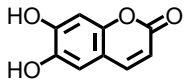	Only trace D_2O or H_2O was determined in DMSO and CH_3CN, respectively. The LOD of H_2O in D_2O was not determined.				Yes	[5]
HTI 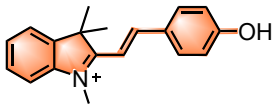	0 – 100	0.19	0.2% DMSO	Dual-modal Ratiometric fluorescent /colorimetric changes	No	**This work**

[a] LR: linear range; LOD: [b] Limit of detection.

Table S3. Photophysical properties of **HTI** and **MTI** in different solvents.

Solution	**HTI**			**MTI**		
	λ_{abs} (nm)	λ_{em} (nm)	ε (cm^{-1} M^{-1})	λ_{abs} (nm)	λ_{em} (nm)	ε (cm^{-1} M^{-1})
H_2O [a]	420/520	515/552	33,700/30,400	416	515	22,800
D_2O [a]	520	558	61,300	416	515	26,700
pH = 3.00 [b]	420	515	38,700	n.d. [c]	n.d. [c]	n.d. [c]
pH = 10.00 [b]	520	558	68,100	n.d. [c]	n.d. [c]	n.d. [c]

[a] Measured in degassed pure H_2O or D_2O; [b] Measured in B-R buffer; [c] Data are not detected.

Table S4. Fluorescence lifetimes of **HTI** (20 μM) in D_2O or H_2O (containing 0.2% DMSO) at 298 K using a bi-exponential function.

	Em	τ_1/ps	Content%	τ_2/ps	Content%	χ^2
D_2O [a]	515 nm	53.87	90.87	710.5	9.13	1.75
	560 nm	51.74	92.63	375.6	7.37	1.30
H_2O	515 nm	42.75	91.81	233.9	8.19	1.35
	560 nm	43.72	91.39	274.9	8.61	1.39

[a] Excited at λex = 400 nm and observed at λem = 515 nm and λem = 560 nm, respectively.

Table S5. Analysis of trace D_2O and H_2O based on the absorbance method.

Sample [a]	Spiked%	Measured%	Recovery%
Trace H_2O in D_2O ($V_{D2O}/V_{D2O+H2O}$)			
1	97.0 [b]	97.3±0.4810 [b]	100.35±0.50
2	95.0 [b]	94.6±0.2244 [b]	99.63±0.24
3	93.0 [b]	92.7±0.1409 [b]	99.68±0.15
4	90.0 [b]	90.4±0.6307 [b]	100.49±0.70
Trace D_2O in H_2O ($V_{H2O}/V_{D2O+H2O}$)			
5	97.0 [c]	97.1±0.3956 [c]	100.07±0.41
6	95.0 [c]	95.0±0.0799 [c]	100.05±0.08
7	93.0 [c]	92.9±0.7348 [c]	99.94±0.79
8	90.0 [c]	90.9±0.6358 [c]	100.97±0.70

[a] Measured in degassed H_2O or D_2O and each sample was measured three times; [b] $V_{D2O}/V_{D2O+H2O}$; [c] $V_{H2O}/V_{D2O+H2O}$.

Table S6. Analysis of trace D_2O and H_2O based on the fluorescent method.

Sample [a]	Spiked%	Measured%	Recovery%
Trace H_2O in D_2O ($V_{D2O}/V_{D2O+H2O}$)			
1	97.0 [b]	97.2±0.3224 [b]	100.22±0.36
2	95.0 [b]	94.3±0.1780 [b]	99.27±0.20
3	93.0 [b]	92.6±0.1048 [b]	99.52±0.12
4	90.0 [b]	89.7±0.5456 [b]	99.68±0.61
Trace D_2O in H_2O ($V_{H2O}/V_{D2O+H2O}$)			
5	97.0 [c]	97.2±0.3224 [c]	100.22±0.36
6	95.0 [c]	94.3±0.1780 [c]	99.27±0.20
7	93.0 [c]	92.6±0.1048 [c]	99.52±0.12
8	90.0 [c]	89.7±0.5456 [c]	99.68±0.61

[a] Measured in degassed H_2O or D_2O and each sample was measured three times; [b] $V_{D2O}/V_{D2O+H2O}$; [c] $V_{H2O}/V_{D2O+H2O}$.

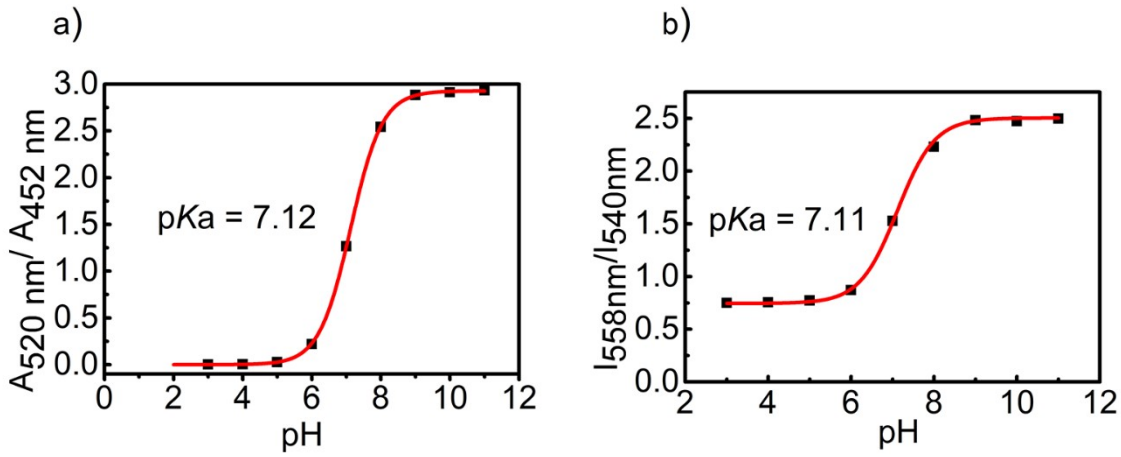

Fig. S1. The relationship of (a) absorption ratio ($A_{520\ nm}/A_{452\ nm}$) and (b) fluorescence ratio ($I_{558\ nm}/I_{540\ nm}$) versus pH values.

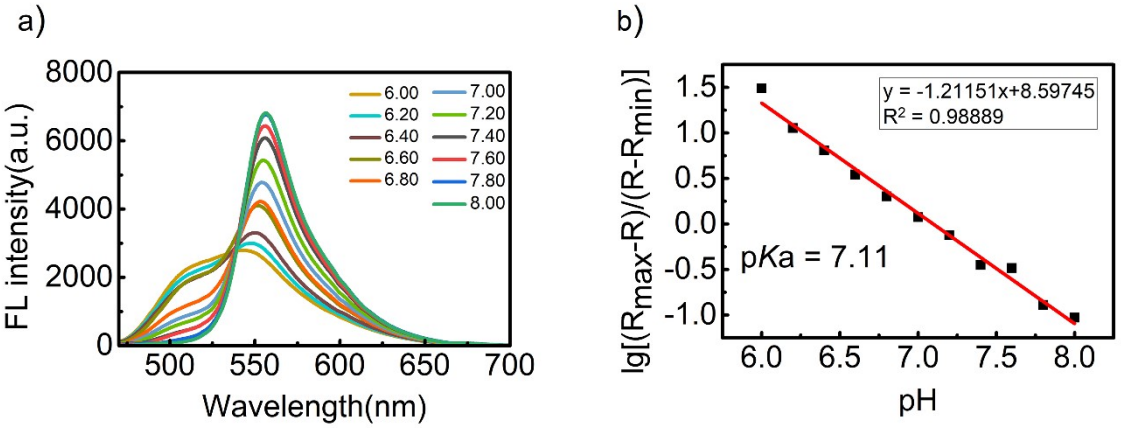

Fig. S2. (a) Fluorescence spectra of **HTI** (20 μM) in B–R buffer (0.2% DMSO) at various pH values (6.0–8.0); (b) Linear relationship between $\lg[(R_{max}-R)/(R-R_{min})]$ and pH values in the range of 6.0 − 8.0; $R = I_{558\ nm}/I_{540\ nm}$.

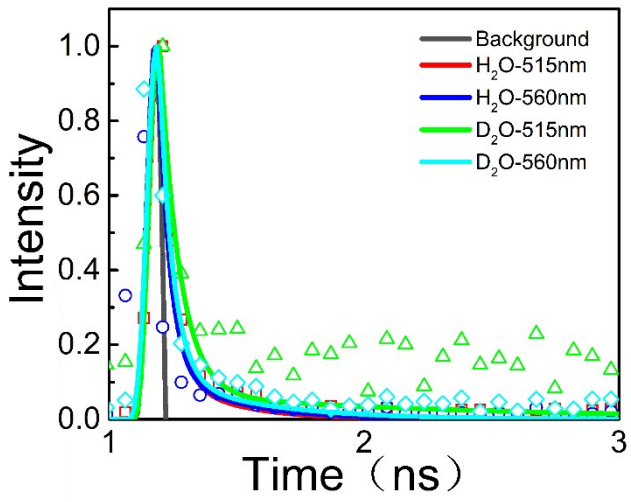

Fig. S3. Fluorescence decay curves of **HTI** (20 μM) in D_2O or H_2O (containing 0.2% DMSO) at 298 K (λex = 400 nm).

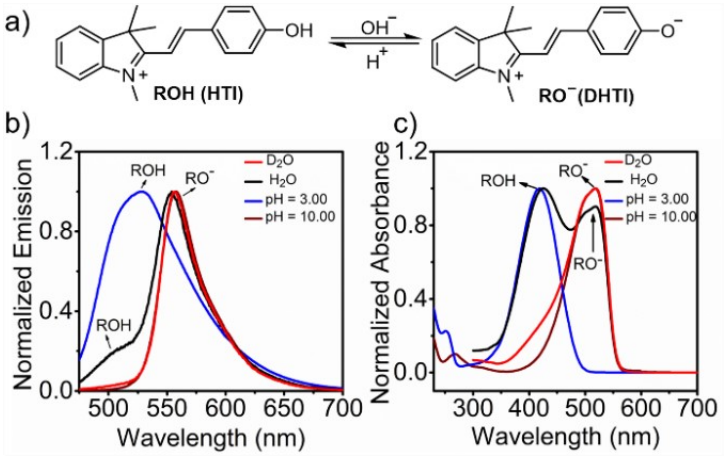

Fig. S4. (a) Proton transfer equilibrium of **HTI** in basic and acidic solutions; (b) Normalized steady-state emission and (c) absorbance spectra of **HTI** (20 μM) in degassed D_2O, H_2O and in solutions with pH = 3.00 and 10.00, containing 0.2% DMSO respectively. Slit: 10 nm/10 nm.

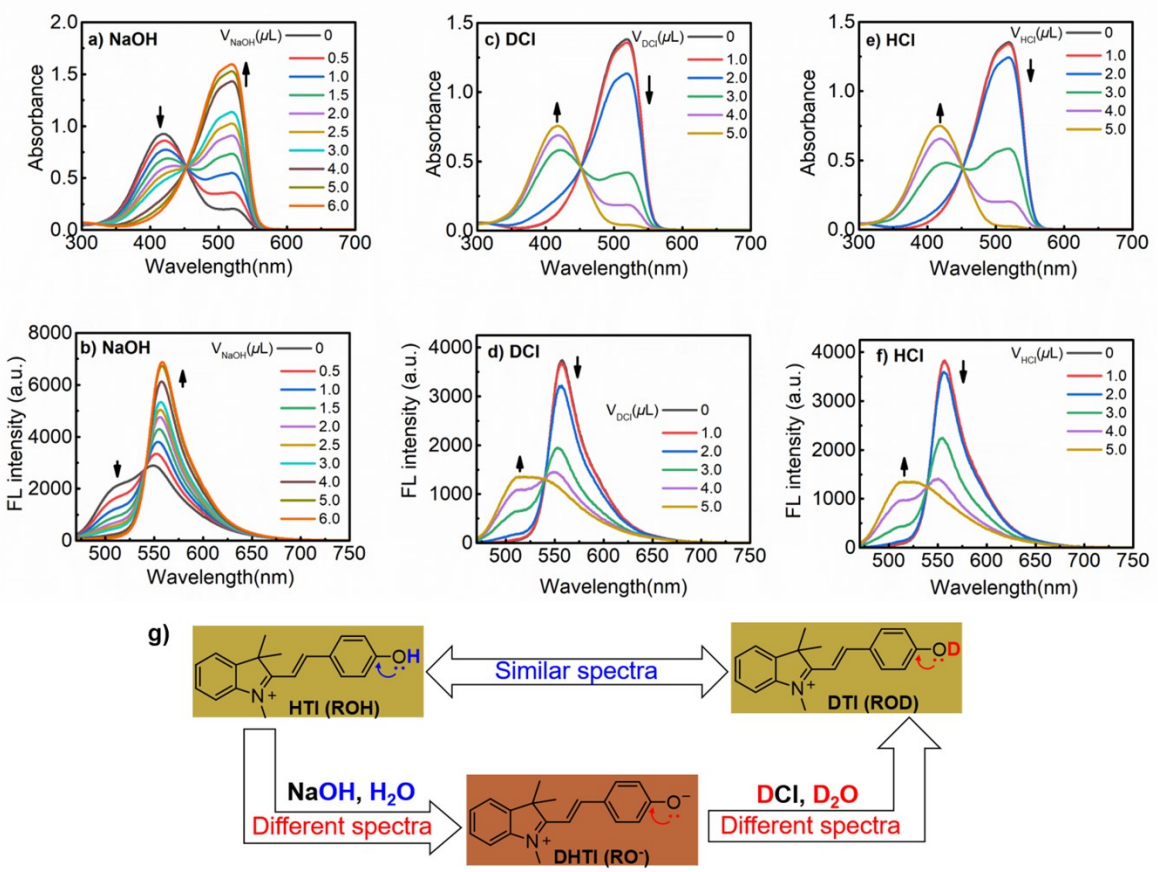

Fig. S5. (a) Absorption and (b) fluorescence spectra of **HTI** (20 μM) in H_2O (0.2% DMSO) with addition of 0.1 M NaOH (0 – 6 uL), Slit: 10 nm/10 nm; (c) Absorption spectra and (d) fluorescence spectra of **HTI** (20 μM) in D_2O (0.2% DMSO) with addition of 0.1 M DCl (0 – 5 uL), Slit: 5 nm/5 nm; (e) UV-vis absorption spectra and (f) fluorescence spectra of sensor **HTI** (20 μM) in D_2O (0.2% DMSO) with addition of 0.1 M HCl (0 – 5 uL), Slit: 5 nm/5 nm; (g) Diagram of related structure transformation.

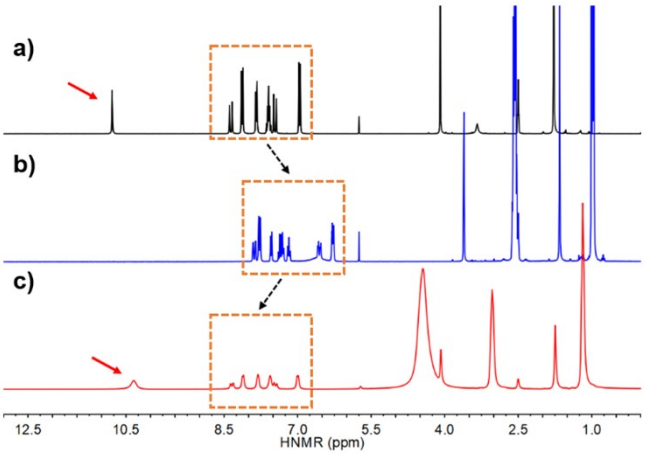

Fig. S6. ^{1}H NMR spectra of **HTI** (0.037 mmol) was conducted in (a) DMSO-d_6, (b) **HTI** with 10 eq. Et_3N (0.37 mmol, 51.3 μL) in DMSO-d_6, and (c) introduce 20 eq. HCl (0.74 mmol, 64.5 μL) into sample b.

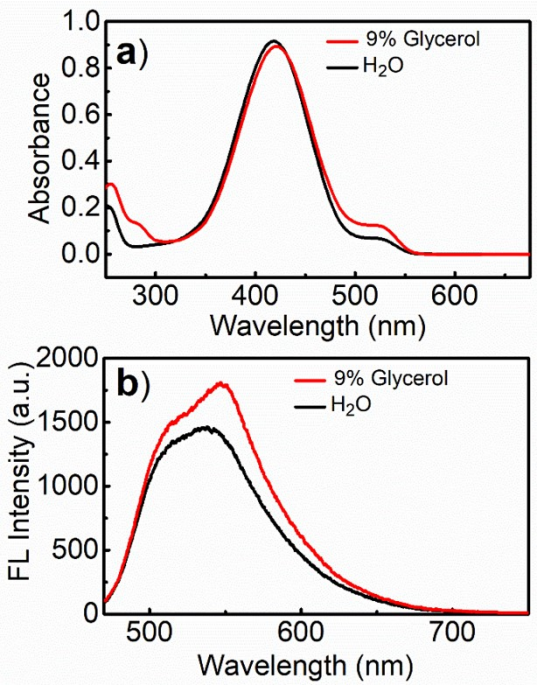

Fig. S7. (a) UV-vis absorption spectra and (b) emission spectra of sensor **HTI** (20 μM) in H_2O (0.2% DMSO) and 9% glycerol (0.2% DMSO).

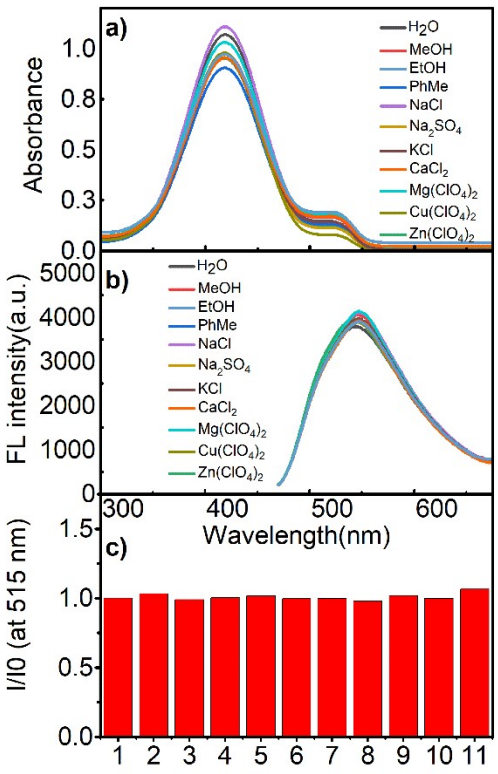

Fig. S8. (a) Absorption and (b) fluorescence spectra of **HTI** (20 μM) in the absence and presence of the other common species (10 eq., 200 μM) in H_2O (0.2% DMSO). (c) Fluorescence responses of sensor **HTI** (20 μM) to common species in H_2O (0.2% DMSO). Bars represent the ratio of the fluorescence intensity in the presence (I) and absence (I_0) of analytes. From 1 to 11: H_2O, MeOH, EtOH, PhMe, NaCl, Na_2SO_4, KCl, $CaCl_2$, $Mg(ClO_4)_2$, $Cu(ClO_4)_2$, $Zn(ClO_4)_2$. Ex = 452 nm.

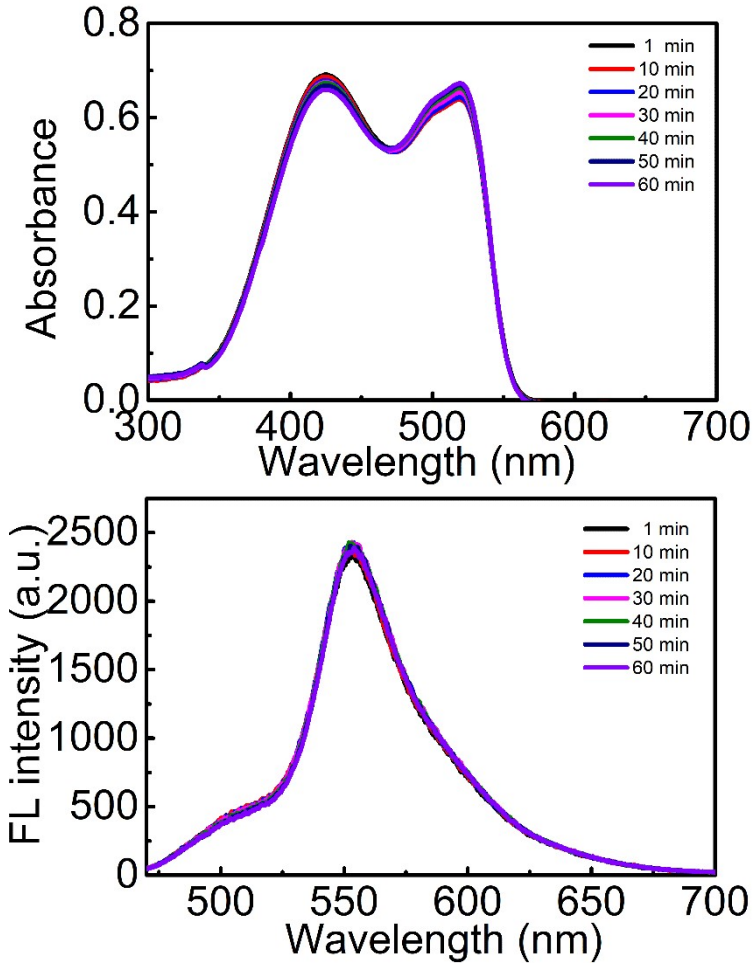

Fig. S9. Fluorescence stability of **HTI** (20 μM) in degassed H_2O (containing 0.2% DMSO). Ex = 452 nm.

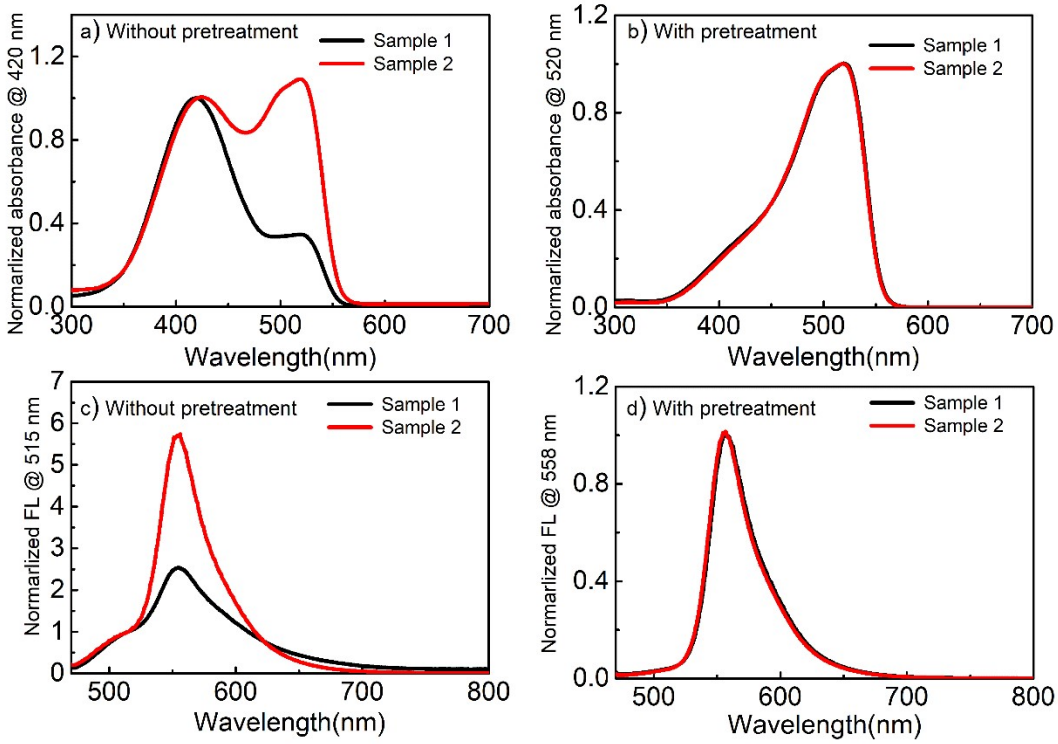

Fig. S10: Normalized absorption (a, b) and fluorescence spectra (c, d) of **HTI** (20 μM) in D_2O (0.2% DMSO) sample 1 (from Energy, China) and sample 2 (from Adamas, China). (a) and (c) represented the sample without pre-treatment and (b) and (d) represented the distilled samples with degas and protection with N_2.

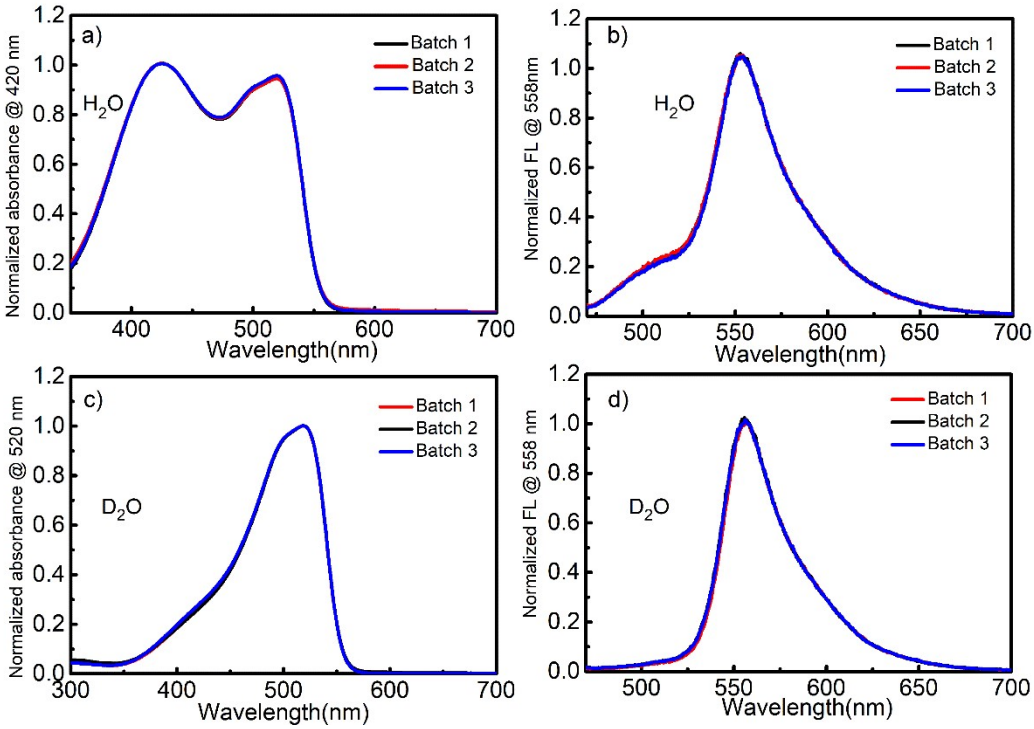

Fig. S11. Consistent absorption (a, c) and emission (b, d) spectra of **HTI** (20 μM) from different batches of degassed H_2O and D_2O, containing 0.2% DMSO. Ex = 452 nm.

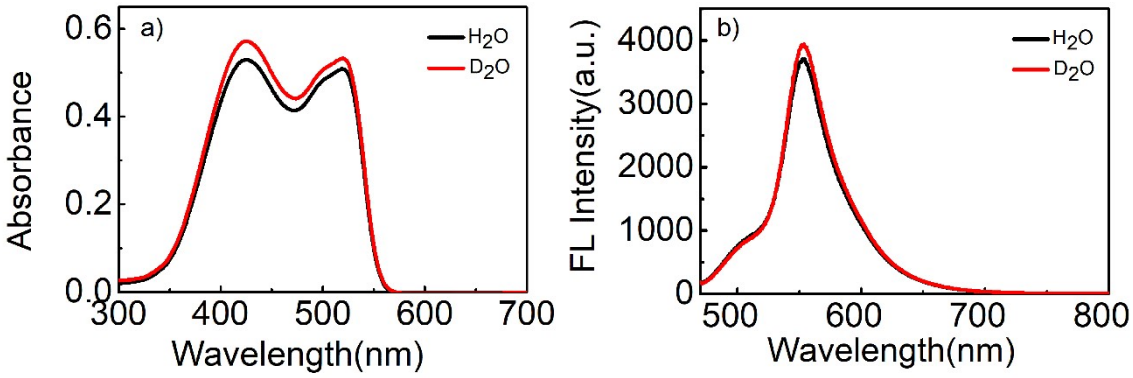

Fig. S12. (a) Absorption and (b) fluorescence spectra of **HTI** (20 μM) in Na_2HPO_4-KH_2PO_4 (10 mM, Na_2HPO_4 : KH_2PO_4 = 1:1) buffer solution in H_2O (black line) and D_2O (red line).

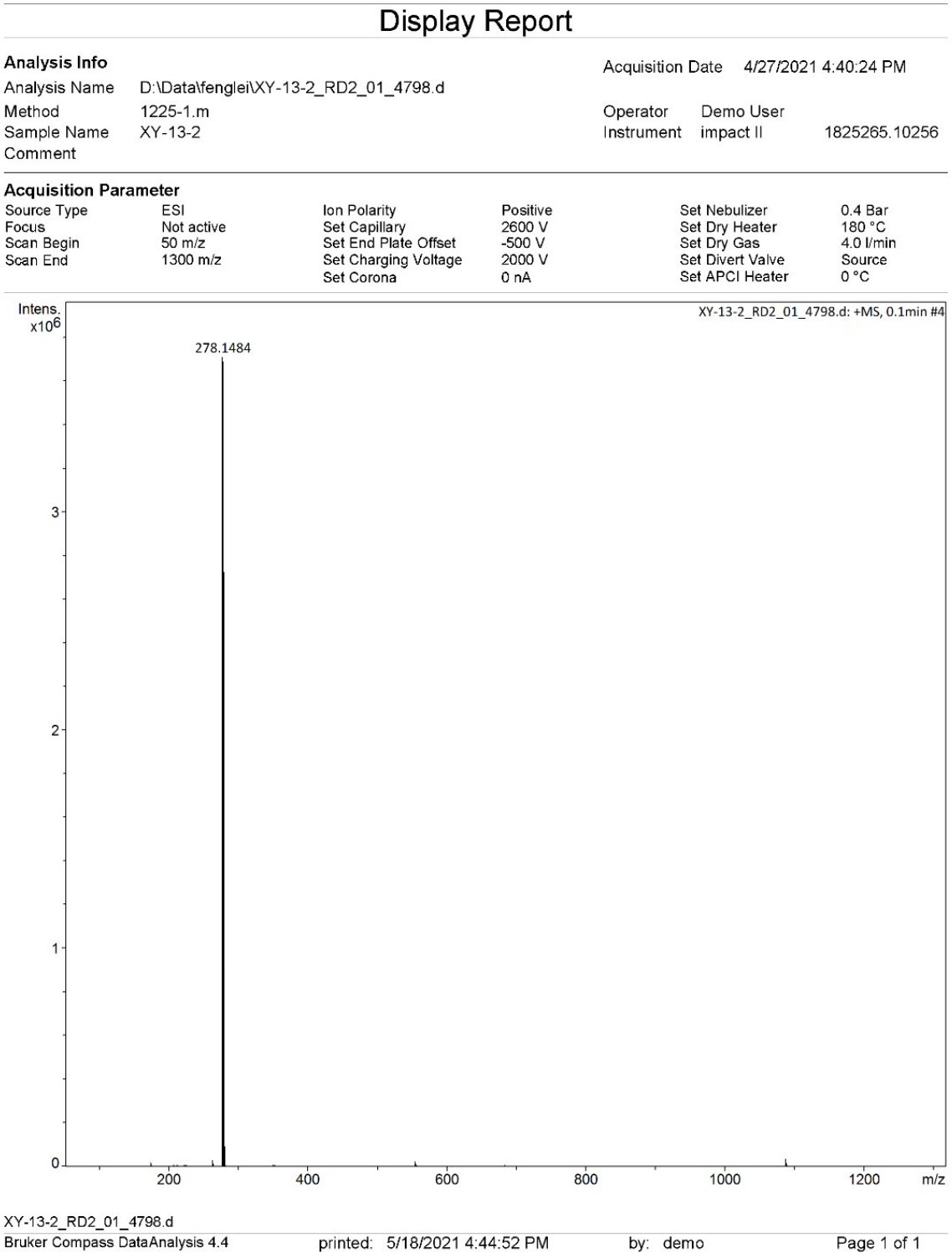

Fig. S13. ESI-MS spectra of **HTI**.

References

1. a) X. Wang, C. Gu, H. Zheng, Y.-M. Zhang, S. X.-A. Zhang, *Chem. Asian J.* **2018**, *13*, 1206; b) S.-P. Wang, W.-J. Deng, D. Sun, M. Yan, H. Zheng, J.-G. Xu, *Org. Biomol. Chem.* **2009**, *7*, 4017.
2. a) A. Perry, *Org. Biomol. Chem.* **2019**, *17*, 4825; b) J. Gu, U. R. Anumala, F. L. Monte, T. Kramer, H. R. Haußen, J. Hölzer, V. Goetschy-Meyer, G. Mall, I. Hilger, C. Czech, B. Schmidt. *Bioorg. Med. Chem. Lett.* **2012,** *22*, 7667.
3. Y. Luo, C. Li, W. Zhu, X. Zheng, Y. Huang and Z. Lu, *Angew. Chem. Int., Ed.* **2019**, *58*, 6280.
4. B. Dong, Y. Lu, W. Song, X. Kong, Y. Sun, W. Lin, *Chem. Commun.* **2020**, *56*, 1191.
5. S. Gadiyaram, P. Kumar, A. Singh, D.A. Jose, *Microchem. J.* **2022**, *176*, 107244.
6. K. A. Rubinson, *Anal. Methods*, **2017**, *9*, 2744.